Received: 2 September 2020 | Revised: 21 April 2021 | Accepted: 21 April 2021

DOI: 10.1096/fj.202002046RR

RESEARCH ARTICLE

THE FASEB JOURNAL

Obesity activates immunomodulating properties of mesenchymal stem cells in adipose tissue with differences between localizations

Camille Lefevre[1,2] | **Dimitri Chartoire**[3] | **Jose Candido Ferraz**[4] | **Thomas Verdier**[1,2] | **Claudie Pinteur**[1,2] | **Stéphanie Chanon**[1,2] | **Sandra Pesenti**[1,2] | **Aurélie Vieille-Marchiset**[1,2] | **Laurent Genestier**[3] | **Hubert Vidal**[1,2] | **Anne Mey**[1,2]

[1]Univ Lyon, CarMeN Laboratory, INSERM U1060, INRAE 1397, INSA Lyon, Université Claude Bernard Lyon 1, Oullins Cedex, France

[2]Hospices Civils de Lyon, Faculté de Médecine, Hôpital Lyon Sud, Oullins Cedex, France

[3]CRCL, Equipe Labellisée Ligue Contre le Cancer, INSERM U1052-CNRS UMR5286, Centre Léon Bérard, Faculté de Médecine Lyon Sud, Université Claude Bernard Lyon I, Oullins Cedex, France

[4]Department of Physical Education and Sports Science, CAV, Federal University of Pernambuco (UFPE), Vitoria de Santo Antão, Brazil

Correspondence
Anne Mey, CarMeN Laboratory, INSERM U1060, INRAE 1397, Batiment CENS-ELI 2D, Hopital Lyon Sud, 165 chemin du Grand Revoyet69921 Oullins Cedex, France.
Email: anne.mey@inrae.fr

Funding information
This study was supported by a grant from INRA-CIRAD: Glofoods programme and from recurrent funding from INSERM, University Lyon I and INRA to the CarMeN laboratory (INSERM U1060-INRA 1397). Camille Lefevre was supported by a PhD fellowship from the French Ministry of Higher Education and Research. Laurent Genestier was supported by The Institute Carnot/CALYM and La Ligue Nationale Contre le Cancer (LNCC)—Equipe Labellisée LIGUE contre le Cancer. Jose Candido Ferraz was supported by the CAPES-COFECUB program. The study funders were not involved in the design of the study; the collection, analysis, and interpretation of data; writing the report; and did not impose any restrictions regarding the publication of the report

Abstract

Mesenchymal stem cells from healthy adipose tissue are adipocytes progenitors with immunosuppressive potential that are used for years in cell therapy. Whether adipose stem cells (ASC) may prevent inflammation in early obesity is not known. To address this question, we performed a kinetic study of high-fat (HF) diet induced obesity in mice to follow the immune regulating functions of adipose stem cells (ASC) isolated from the subcutaneous (SAT) and the visceral adipose tissue (VAT). Our results show that, early in obesity and before inflammation was detected, HF diet durably and differently activated ASC from SAT and VAT. Subcutaneous ASC from HF-fed mice strongly inhibited the proliferation of activated T lymphocytes, whereas visceral ASC selectively inhibited TNFα expression by macrophages and simultaneously released higher concentrations of IL6. These depot specific differences may contribute to the low-grade inflammation that develops with obesity in VAT while inflammation in SAT is delayed. The mechanisms involved differ from those already described for naïve cells activation with inflammatory cytokines and probably engaged metabolic activation. These results evidence that adipose stem cells are metabolic sensors acquiring an obesity-primed immunocompetent state in answer to depot-specific intrinsic features with overnutrition, placing these cells ahead of inflammation in the local dialog with immune cells.

KEYWORDS

adipose tissue, immune regulation—immunometabolism, low-grade inflammation, mesenchymal stem cells, obesity

Abbreviations: ASC, adipose stem cells; CTV, cell trace violet; FoxP3+ Treg, regulatory T lymphocytes expressing FoxP3; HF diet, high-fat diet; LPS, lipopolysaccharides; RS17, ribosomal protein S17; RT-qPCR, real-time quantitative PCR; SAT, subcutaneous adipose tissue; S-ASC, subcutaneous adipose stem cells; SD diet, standard diet; TBP, TATA-Box Binding Protein; VAT, visceral adipose tissue; V-ASC, visceral adipose stem cells.

1 | INTRODUCTION

Inflammation plays a central role in the risk associated with obesity for the development of metabolic complications such as type 2 diabetes,[1] and for inflammatory complications in viral infections.[2] Preceding complications, obesity promotes a chronic and low-grade inflammation supplied by several organs[3] including visceral adipose tissue,[4,5] and triggered by hyperglycemia, fatty acids excess[6,7] or by pro-inflammatory factors released by the gut.[8] This correlates with fat deposition in visceral adipose depots,[9,10] that is balanced by the protective energy storage in subcutaneous depots. Complications occur as the expansion of subcutaneous adipose tissue (SAT) has reached a limit[11] and, in turn, becomes a major contributor to systemic inflammation.[12,13] Therefore, the control of adipose tissue inflammation is challenging to prevent complications in obesity.

In the stroma of white adipose tissue, adipose stem cells (ASC) are adipocyte progenitors.[14] Belonging to the mesenchymal stem cell's family (MSC), they also have a broad range of immunosuppressive properties towards activated T and B lymphocytes, macrophages and dendritic cells, allowing their use in transplantation to prevent graft rejection.[15] Loss of resident regulatory T[16] and B lymphocytes[17] that support immunosuppressive functions, is a primary cause of obesity-induced inflammation[18] that promotes the metabolic syndrome.[19] In parallel, macrophage infiltration occurs, starting in visceral adipose tissue (VAT) with a higher intensity than in SAT.[20] Human ASC isolated from obese adipose tissue present adipogenic[21] and immune[22] dysfunctions, but the contribution of ASC to the immune cell remodeling that precedes inflammation in adipose tissue during early obesity is not known.

To address this question, we performed a kinetic study of diet-induced obesity in mice and analyzed changes in ASC immune properties at progressive stages of metabolic alterations and inflammation. Our results reveal that ASC from SAT and VAT (respectively S-ASC and V-ASC) are both early responding to obesogenic diet, with differences between adipose depots in the control of macrophages and of activated T lymphocytes. These data place ASC activity in the immune adaptation of adipose depots to obesity.

2 | MATERIALS AND METHODS

2.1 | Animal protocol

Mouse studies were performed in accordance with the institutional guidelines for the care and use of laboratory animals and with the approval of the Regional Committee of Ethics for Animal Experiments. Mice were C57BL/6J 5-week-old male, purchased from Envigo (Gannat, France). After a week acclimatization, the mice were fed with a high-fat (HF) diet containing 16.6% sucrose (MD.99249, 36% fat diet, Envigo, France) or with a standard diet (SD) (LASQCdiet® Rod16-R, LASvendi, France) for 6, 10 and 14 weeks (Figure 1). The body weight was monitored weekly. Mice were killed by cervical dislocation and blood, spleen, inguinal (subcutaneous, SAT) and epididymal (visceral, VAT) adipose tissues were collected. We used 8 animals per group and per time, randomly distributed into 2 cages. The kinetic study was performed one time from 6 to 10 weeks feeding and two times from 6 to 14 weeks feeding. They gave similar metabolic changes in mice but results with cells are from one protocol where samples were treated individually.

2.2 | Glucose metabolism analysis

The week preceding sacrifice, glucose tolerance test (GTT) and insulin tolerance test (ITT) were performed on randomized mice from distinct cages. GTT was performed by an intraperitoneal injection of 2 mg/g body weight of glucose in 16 hours fasted mice. For ITT, 0.75 mU/g of insulin (NovoRapid, France) was injected to 6 hours fasted mice. After injections, glycemia was monitored every 15 minutes for 90 and 60 minutes, respectively using an Accu-Chek (Roche, France) glucose meter.

2.3 | Circulating blood dosages

Circulating levels of IL6, MCP1, TNFα, PAI-1, resistin, and leptin were measured using Milliplex technology (MADCYMAG-72K Millipore, France). Insulinemia was measured by ELISA using a mouse ultrasensitive kit (ALPCO, France). The circulating triglyceride levels were analyzed with the GPO detection kit (BIOLABO, France). Circulating free fatty acids were measured using the free fatty acids quantification kit (SIGMA Aldrich, France) according to manufacturer's instructions.

2.4 | Histology

Immediately after collection, SAT and VAT were fixed in 4% formaldehyde, before paraffin embedding. Slices of 4 µm section were deparaffinized and heated in 10 mM citrate buffer for antigen retrieval. Macrophages and T lymphocytes were detected using a monoclonal rat anti-mouse F4/80 (Novus Biologicals, Minneapolis, USA) or polyclonal rabbit anti-CD3 (Agilent, Santa Clara, CA, USA) and DAB reaction followed by counterstaining with hematoxylin. Non-deparaffinized slices were illuminated with FITC filter and autofluorescence of adipocytes was used for determination

of adipocytes area. An upright microscope (Olympus BX63) and Cellsens imaging software (Olympus) were used for image captures with a 200x magnification. At least 250 adipocytes from random fields were observed and counting used Fiji application.

2.5 | Isolation, culture, and adipogenic differentiation of adipose stem cells from SAT and VAT

Procedures have been described previously.[23] Cultured cells used in this study were at the third passage after seeding of the stromal vascular fraction. Cells were free of mycoplasma as tested using the MycoAlert detection kit (Lonza).

2.6 | Flow cytometry

The labeling procedure and antibodies have previously been described.[23] PE anti-mouse CD274/PD-L1 antibody was from Biolegends (France). On the stromal vascular fraction the ki67 PerCP-eFluor 710 antibody from Life technologies (Thermo Fisher, France) was added. Acquisitions were performed using an LSRII flow cytometer from the platform AniRA of the SFR Biosciences Gerland-Lyon Sud. Analyses were performed using Cytobank (https://cytobank.org).

2.7 | Isolation of T lymphocytes

Spleen and lymph nodes (mesenteric, inguinal, brachial and axillary) were dissociated in digestion buffer (1 mg/ml collagenase 1A), 0.1 mg/mL DNAse (all from Sigla Aldrich, France), 2% FBS in RPMI (Dominic Dutscher, France) for 30 minutes at 37°C under agitation. Digestion was stopped with PBS containing 2% FBS and 2% Hepes and cells were passed through a 100-µm nylon filter. After centrifugation, the red blood cells in the pellet were lysed using ACK lysing buffer (155 mM ammonium chloride, 10 mM potassium bicarbonate, 0.1 mM EDTA). After washing, cells were suspended in RPMI culture medium (1% glutamine, 10% FBS, 2% Hepes, 100 U/mL penicillin, 100 µg/mL streptomycin) and numbered before negative selection of T cells on column using the Pan T cell isolation kit II, mouse (Miltenyi, France).

2.8 | Lymphocyte proliferation test in coculture with ASC

Co-culture experiments were performed in triplicates in 96-well dishes (Falcon, France). ASC were plated at 42 000 cells/well in 100 µL DMEM HG culture medium (DMEM high glucose, 10% FBS, 100 U/mL penicillin, 100µg/ml streptomycin, 2 mM glutamine) and cultured 24 hours at 37°C, 5% CO_2. Medium was removed and replaced by CTV-labeled T cells supplemented with CD3/CD28 activation beads at 200 000 cells/well in RPMI 10% FBS, 100 U/mL penicillin, 100 µg/mL streptomycin, 2mM glutamine. Co-cultures were maintained for 72 hours and CTV dilution was acquired on LSRII flow cytometer as indicated above. Analyses were performed using the FlowJo software.

2.9 | Migration tests with T lymphocytes

Purified T lymphocytes at 1 million/ml were activated with coated anti-CD3+ antibody (BE0001-1 clone 145-2C11, Bio BioXcell, France) in combination with 1 µg/mL soluble anti-CD28+ in RPMI culture medium for 72 hours at 37°C. Resting T lymphocytes were prepared the day of co-culture launching. ASC were plated at 80 000 cells/well/mL of DMEM culture medium in 24-well dishes (Falcon, France). After 24 hours, medium was replaced by 600 µL of 1.5% FBS RPMI medium (100 U/mL penicillin, 100 µg/mL streptomycin, 2 mM glutamine) and a 5-µm porosity Transwell (Costar, France) insert was placed in the well. Activated or resting T lymphocytes at 200 000 cells in 100 µL of 3% FBS RPMI culture medium, supplemented with 10 ng/mL IL2 (Peprotech, France) for activated LyT, were placed in the Transwell insert and the cells were cultured for 12 hours. For analysis, a quart of the volume in the lower chamber was collected for counting migrated cells. Propidium iodide solution (Biolegend, France) was used to exclude dead cells and viable cells were numerated with attune NXT (Thermo fisher, France). The other part of the migrated cells was incubated with the fixable viability dye efluor 780 (65-0865-14, Biosciences, France) to exclude dead cells and next incubated with anti-CD4, anti-CD8, anti-CD25, and anti-FoxP3 antibodies for phenotyping of the migrated T cells.

2.10 | Phenotyping of the migrated T lymphocyte population

Cells were marked with anti-CD4+ (BV605 Biolegend 100547 clone RM4-5, France), anti-CD8+ (BV786 563332 clone 53-6.7, BD Horizon, France), anti-CD25+ (BV421 562606 clone PC61, BD Horizon, France), anti-CD62L+ FITC (11-0621-81 clone Mel-14, ebioscience, France), anti-CD3+ PE (CF594 562286 clone 145-2C11, BD Horizon, France), anti-CD69+ Percp-Cy5.5 (551113 clone 3F3, BD Pharmingen, France), anti-CD44+ APC (559250 clone IM7, BD Pharmingen, France) in FACS buffer (PBS, 2% SVF, 0.5 mM EDTA, 0.01% azide. Cells were then fixed and permeabilized with FoxP3 transcription factor staining buffer kit (00-5523-00) and cells

were marked with anti-Foxp3 (12-5773-82, PE eBioscience, France) according to the recommendations of the manufacturer. Acquisitions were performed with flow cytometer and analyses using the Cytobank platform.

2.11 | Migration test with macrophages

RAW 264.7 cells were cultured in DMEM HG culture medium. ASC were plated at 80 000 cells/well/mL of DMEM HG culture medium in 24-well dishes. After 24 hours, medium was replaced by 600 µL of 3% SVF DMEM HG (100 U/mL penicillin, 100 µg/mL streptomycin, 2 mM glutamine) and a 5 µm porosity Transwell insert was placed in the well. RAW264.7 macrophages were placed in the insert at 200 000 cells in 100 µL of DMEM HG without FBS and the cells were cultured for 24 hours at 37°C, 5% CO_2. Each condition was tested using Transwell duplicates. Migrated RAW cells accumulated at the lower face of the Transwell membrane. Their nucleus was labeled by incubation 30 minutes at 37°C in 1/1000 Hoechst (Sigma Aldrich) added to the culture. Next, the cells were fixed for 10 minutes in 3.7% formaldehyde and washed twice with PBS. The cells on the upper surface were removed with a cotton bud. Migrated cells were counted at the lower surface of the insert using fluorescence microscopy. Results are from two independent experiments using a total of ASC samples from 6 distinct mice per group. Ten images in the first experiment and at least 120 images per insert in the second one, were captured at a ×20 magnification to cover all the surface. Images were analyzed using the ImageJ software. The mean number of migrated RAW per field was measured and compared to the spontaneous migration of RAW in the presence of medium alone.

2.12 | Culture of activated macrophages with ASC-conditioned media

ASC-conditioned media were prepared by cultivating sub confluent ASC in 6-wells dish in 2ml DMEM HG culture medium for 18h. Conditioned media were stored at −80°C until use. RAW cells were activated using LPS (1 µg/mL) from Salmonella typhimurium (Sigma Aldrich, France) for 24 hours (M1 like polarization) before replacement with fresh medium supplemented with ASC-conditioned media (vol/vol). After 24 hours culture, the RAW cells were collected in RNA lysis buffer for RNA extraction.

2.13 | Cytokines quantification by ELISA

IL6, PGE2, M-CSF, and IL10 in ASC-conditioned media were analyzed in duplicates using DuoSet ELISA kit for the expression of mouse IL6, IL10, TNFα and TGFβ1 and Quantikine ELISA kits for the expression of mouse PGE2 and M-CSF, all were from R&D systems, France. Culture medium was used as negative control and concentration deduced from the results obtained with conditioned media.

2.14 | Real-Time Quantitative PCR (RT-qPCR)

After RNA extraction and reverse transcription, gene expression levels were measured by quantitative PCR and calculated using the RotorGene Q series software. They were normalized on housekeeping genes that were the mouse 40S ribosomal protein S17 (RS17) for adipose stem cells and adipose tissue, and the TATA-Box Binding Protein (TBP) for RAW 264.7 cells. Primers are listed in Table 1 and procedures have been previously described.[23]

2.15 | Statistics

All results are means ± SEM of data from distinct animals analyzed individually. In the figures, each point is the mean of the technical replicates. Two-way ANOVA followed by Sidak's multiple comparisons test or one-way ANOVA followed by Dunnett's multiple comparison test were used to evaluate the probability of significant differences. A P-value $<.05$ was considered as significant. We mentioned as tendency the situation where significant difference was associated with one (or two) variable in ANOVA, but not in the comparisons by pairs. GraphPad Prism software was used for all statistical analysis.

3 | RESULTS

3.1 | Metabolic alterations and inflammation are sequencing events in increased obesity

The kinetic protocol performed in this study is presented in Figure 1A. Male C57BL/6J mice were fed for 6, 10 or 14 weeks with standard (SD) or high fat (HF) diet.

3.1.1 | Metabolic status of mice

HF diet induced the expected body weight gain (Figure S1A) that was significant from 5 weeks of feeding. Fasting glycemia (Figure 1B) and glucose tolerance test (Figures 1C and S1B) performed one week before sacrifice showed alterations of the glucose metabolism from 5 and 9 weeks of HF diet respectively

TABLE 1 List of primers used in qPCR

Genes	Forward sequence (5′ → 3′)	Reverse sequence (5′ → 3′)
TBP	TGGTGTGCACAGGAGCCAAG	TTCACATCACAGCTCCCCAC
RS17	CATTATCCCCAGCAAGAAGC	CTGAGACCTCAGGAACGTAG
Leptin	TGGTGTGCACAGGAGCCAAG	TTCACATCACAGCTCCCCAC
Adiponectin	AGGCCGTGATGGCAGAGATG	CTTCTCCAGGTTCTCCTTTCCTGC
PPARγ	TCTCTCCGTAATGGAAGACC	GCATTATGAGACATCCCCAC
DGAT2	AAGGGCTTTGTGAAACTGGC	CCTCCTCGAAGATCACCTGC
FAS	GTGCACCCCATTGAAGGTTCC	GGTTTGGAATGCTGTCCAGGG
TNFα	CCAGACCCTCACACTCAGATC	CACTTGGTGGTTTGCTACGAC
IL6	AGTTGCCTTCTTGGGACTGAT	TCCACGATTTCCCAGAGAAC
IFNγ	GCGTCATTGAATCACACCTG	TGAGCTCATTGAATGCTTGG
IL1β	ACTGTTCCTGAACTCAACTG	CTTGTTGATGTGCTGCTGCG
IL10	CAGGGCCCTTTGCTATGGTG	CGGCTGGGGGATGACAGTAG
Ccl2 (MCP1)	TGGAGCATCCACGTGTTGGC	ACTACAGCTTCTTTGGGACA
Ccl5	TCAAGGAGTATTTCTACACCAG	TGGCACACACTTGGCGGTTC
Cxcl9	CTACAAATCCCTCAAAGACCT	CCCATTCTTTCATCAGCTTC
Cxcl10	GACTCAAGGGATCCCTCTC	ATGGCCCTCATTCTCACTG
Cxcl12	AGTCAGCCTGAGCTACCGAT	CCAGGTACTCTTGGATCCAC
Cxcl1	AATGAGCTGCGCTGTCAGTG	CTTGAGTGTGGCTATGACTTCG
i-NOS	ACACACAGCGCTACAACATC	CGGTACTCATTCTGCATGTG
PTGS2	CTGCGCCTTTTCAAGGATGG	TCCTGCCCCACAGCAAAC
M-CSF	CTGCTTCACCAAGGACTATG	AGAGCACTTAGCAAAGCTGT
GM-CSF	TGAACATGACAGCCAGCTAC	AGTTCCTGGCTCATTACGCA
CD274	AATGTGACCAGCAGTCTGAG	AAGCACCCAGTGAGTCCTGT
TGFβ	AGGGCTACCATGCCAACTTC	GGTTGTGTTGGTTGTAGAGG
HGF	ATCAGGAACAGGGGCTTTACG	TGGAATTCCAAGGCTGGCAT
ARG1	GTGAAGAACCCACGGTCT	CTGGTTGTCAGGGGAGTGTT

and insulin resistance was obtained only after 13 weeks of feeding in accordance with the increased fasting insulinemia (Figure 1D) and as assessed by the insulin tolerance test (Figure 1E and Figure S1C). Lipid metabolism was moderately altered, with fed circulating levels of triglycerides and free fatty acids showing slight modifications not consistent over the different time-points of the protocol (Figure 2D). However, ANOVA indicated the significant influence of the feeding duration (Time **) on both markers in addition to the type of diet (Diet*) for FFA. A longer exposure to HF feeding would probably show more consistent alterations. These results indicated that there was no systemic alterations of lipid metabolism and no major metabolic defect of adipose tissue metabolic functions at this stage of early obesity.

3.1.2 | Secreting function of adipose tissue

White adipose tissue weight gain (Figure 2A) was significant from 6 weeks of feeding. Hypertrophic adipocytes were observed in SAT adipose tissues at sacrifice from 6 weeks of HF feeding (Figure 2B), confirming the progress towards metabolic complications.[24] RT-qPCR results showed increased expression of the pro-inflammatory *leptin* from 6 weeks of HF diet in VAT (Figure 2C). Accordingly, the circulating levels of leptin secreted by the white adipose tissue was increased from 6 weeks of HF feeding, circulating resistin was increased also (Figure 2D) but circulating adiponectin mainly produced by subcutaneous adipocytes and measured by ELISA on three samples was not changed (data not shown). These changes are typical of an unaltered adaptative metabolic response of adipose tissue to obesity.

3.1.3 | Inflammatory status

In the plasma, the concentrations of inflammatory cytokines (IL6, MCP1, TNFα) were below the detection limit but PAI-1 (plasminogen activator inhibitor-1), that signals an increased risk of insulin resistance,[25] was increased

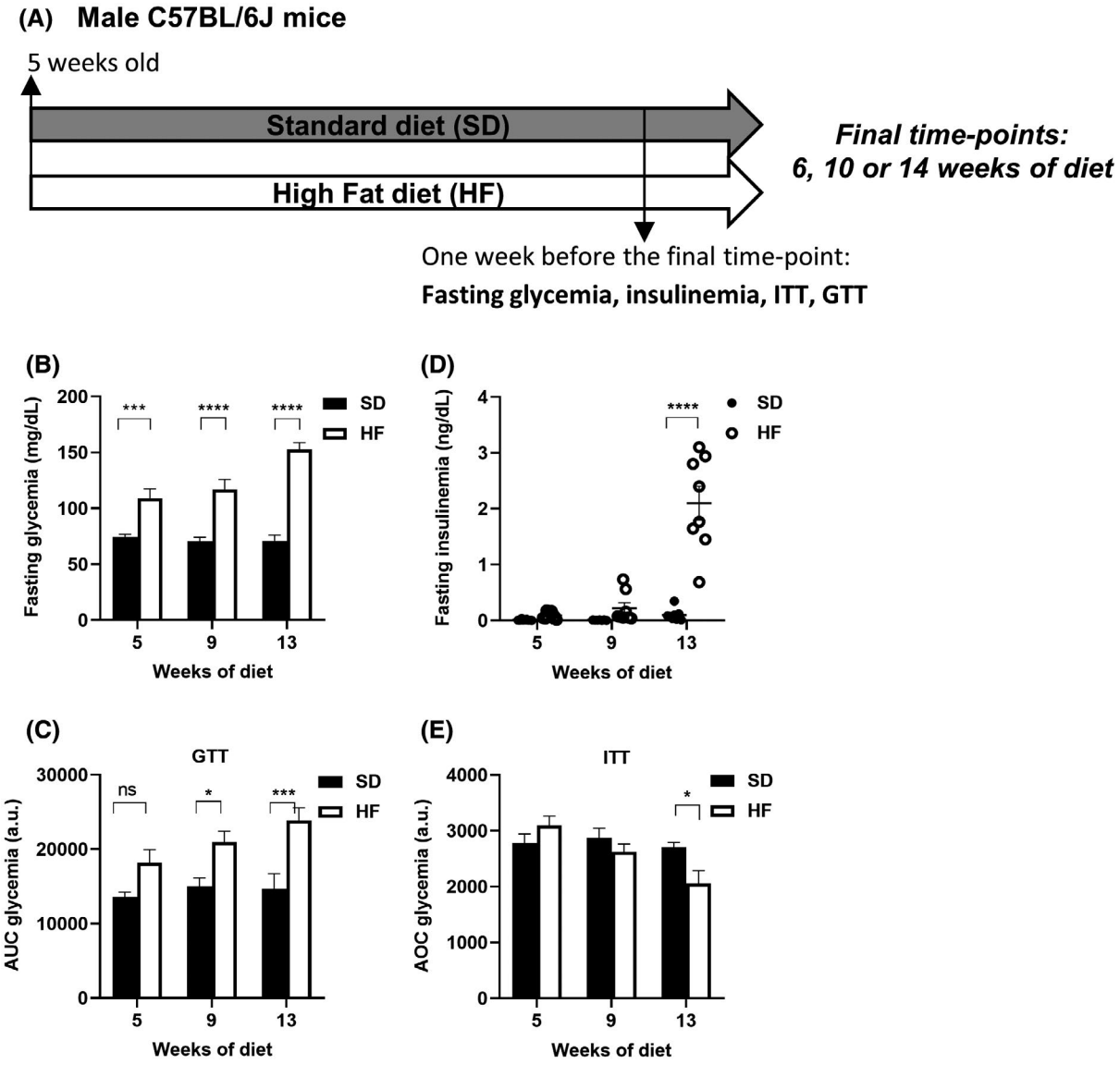

FIGURE 1 Glucose metabolism was altered from 6 weeks of high fat feeding: A, Scheme of the animal protocol used. B, Fasting glycemia measured the week preceding sacrifice. C, Area under the curve in GTT assay performed after 5, 9 and 13 of diet. D, Fasting insulinemia. E, Area under curve in ITT assay performed after 5, 9 and 13 of diet. Results are from 8 mice per group of diet and per time. Results are means ± SEM. Statistics are from two-way ANOVA followed by Sidak's test for multiple comparisons: $****P < 10^{-4}$, $***P < 10^{-3}$, $*P < .05$, ns: not significant

from 10 weeks of HF diet (Figure 2D). To detect local inflammation, the expression of pro-inflammatory cytokines was measured in SAT and in VAT by RT-qPCR. The expression of *TNFα* was significantly increased in VAT after 10 weeks of HF diet but not in SAT (Figure 3B, A respectively). The expression of the other main pro-inflammatory cytokines, *IL6* and *IFNγ*, and of the anti-inflammatory cytokine *IL10* were not changed in neither of the two depots (Figure 3A,B).

Expanding adipose tissue in obesity is known to recruit immune cells in the phases preceding inflammation.[20] Accordingly, the expression of chemokines was increased in SAT (*Cxcl12*) and in VAT (*Ccl2*) from 6 weeks of feeding (Figure 3C,D, respectively).

Immunohistochemical analysis was performed using anti-CD3 and anti-F4/80 antibodies to observe in adipose tissue the infiltration with T lymphocytes and macrophages, respectively (Figure 3E). In VAT, macrophages surrounding dead adipocytes in crown-like structures.[26] were observed in many microscopic fields from 10 weeks of HF diet. No difference was seen between SD and HF conditions when examining T lymphocytes in VAT, nor for any of the two cell types in SAT. Flow cytometry analysis of freshly isolated adipose tissue confirmed that macrophages and T lymphocytes co-expressing the hematopoietic cells marker CD45 with the F4/80 and CD3 antigen, respectively, were present at the same proportions between SD and HF diet conditions. This conclusion was the same after 6 and 10 weeks of feeding in both SAT and VAT (Figure 3F).

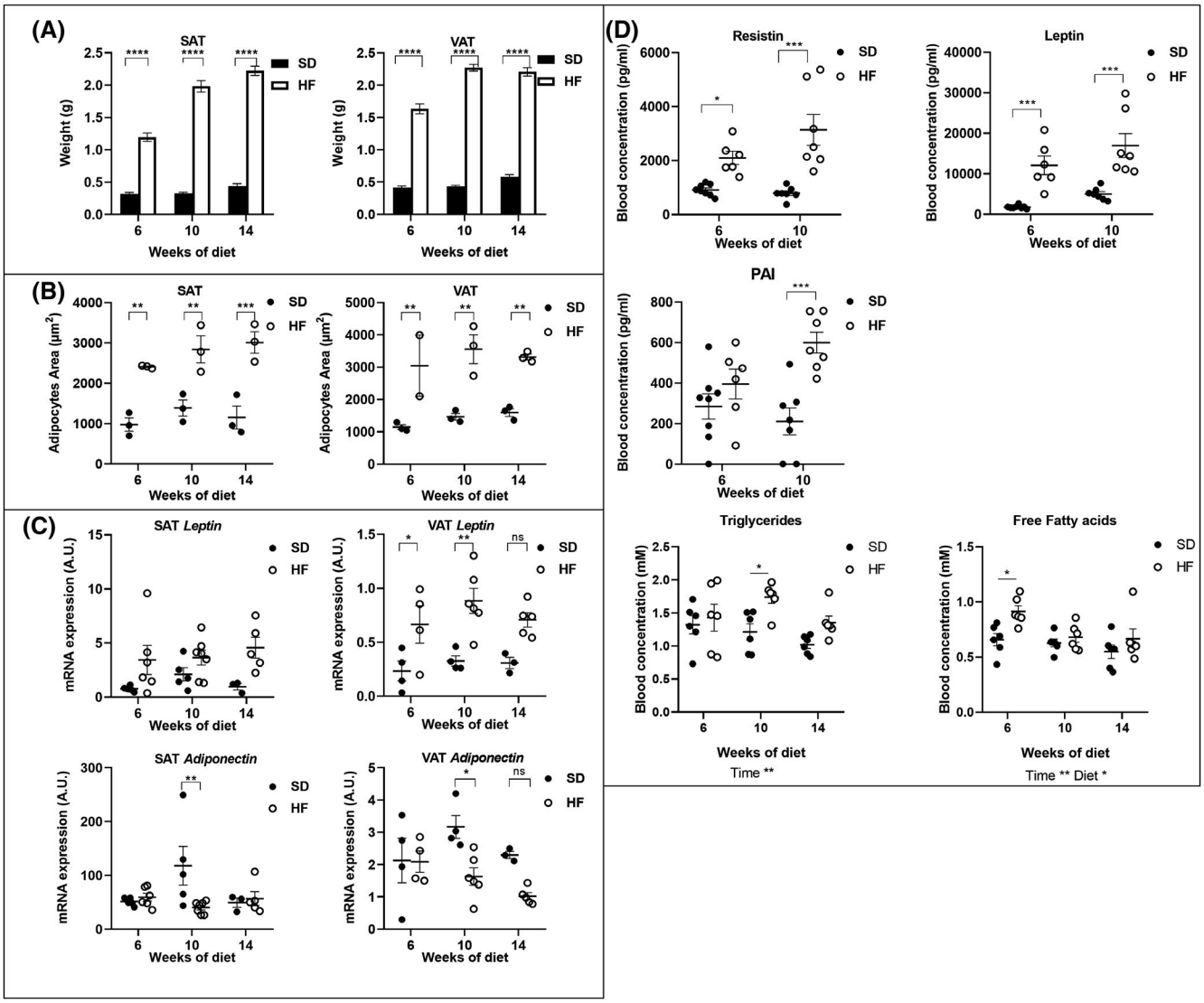

FIGURE 2 Hypertrophic adipocytes and altered adipokines levels, but not inflammatory cytokines, were induced by HF diet: Results from sub-cutaneous (SAT, left column) and visceral adipose tissues (VAT, right column) are represented (in A to C). A, Adipose tissue weight gains, mean ± SD from n = 18 mice per group. B, Adipocytes area measured on paraffin sections of adipose tissues. Each point represents one animal (n = 4) and is the mean surface of 200 adipocytes. C, *Leptin* and *Adiponectin* mRNA levels, quantified by RT-qPCR. Values were normalized on the expression level of the RS17 gene and are relative to an internal standard curve in arbitrary units (AU). Mean ± SEM of n = 4 to 6 distinct mice. D, Circulating level of resistin, leptin, PAI-1, triglycerides and free fatty acids at the indicated time of feeding in the plasma of fed mice. Circulating MCP1, TNFα, and IL6 were below the detection level of the Milliplex method used and are not represented. Mean ± SEM from n = 3 to 8 animals. Statistics are from two-way ANOVA followed by Sidak's test: $****P < 10^{-4}$, $***P < 10^{-3}$, $**P < .01$, $*P < .05$, n.s. not significant. Times** indicates the influence of the feeding time ($P < .01$) and Diet* the influence of thediet ($P < .05$) in two-way ANOVA

Therefore, the crown-like structures observed by immunohistochemistry (Figure 3E) reflected local changes with obesity, in the distribution of resident macrophages in VAT. B lymphocytes were not detected using anti-CD19 antibodies (Figure 3F), nor with anti-IgM or anti-B220 antibodies (data not shown). Macrophages represented the majority of the CD45 positive cells after 6 and 10 weeks of feeding but the proportion of T lymphocytes increased from 10 weeks of feeding independently of the diet. It is of note that this increase was lower with HF than with SD diet in both SAT and VAT, but this difference was not statistically significant.

Therefore, the kinetic protocol performed in this study was representative of adipose tissue adaptation to energy excess in early obesity. We next assessed changes affecting ASC.

3.2 | HF diet does not alter the proliferation and the differentiation potential of ASC in vitro

ASC were obtained by the seeding of enzymatically dissociated adipose tissue depleted from adipocytes. After three

passages, we used flow cytometry analysis to look for the expression of hematopoietic (CD45) and endothelial (CD31) cell lineages markers, and for the expression of mesenchymal stem cells markers CD29 and CD90 (Figure 4A). The culture conditions efficiently discarded the hematopoietic and the endothelial cells with 100% of the cells being negative for

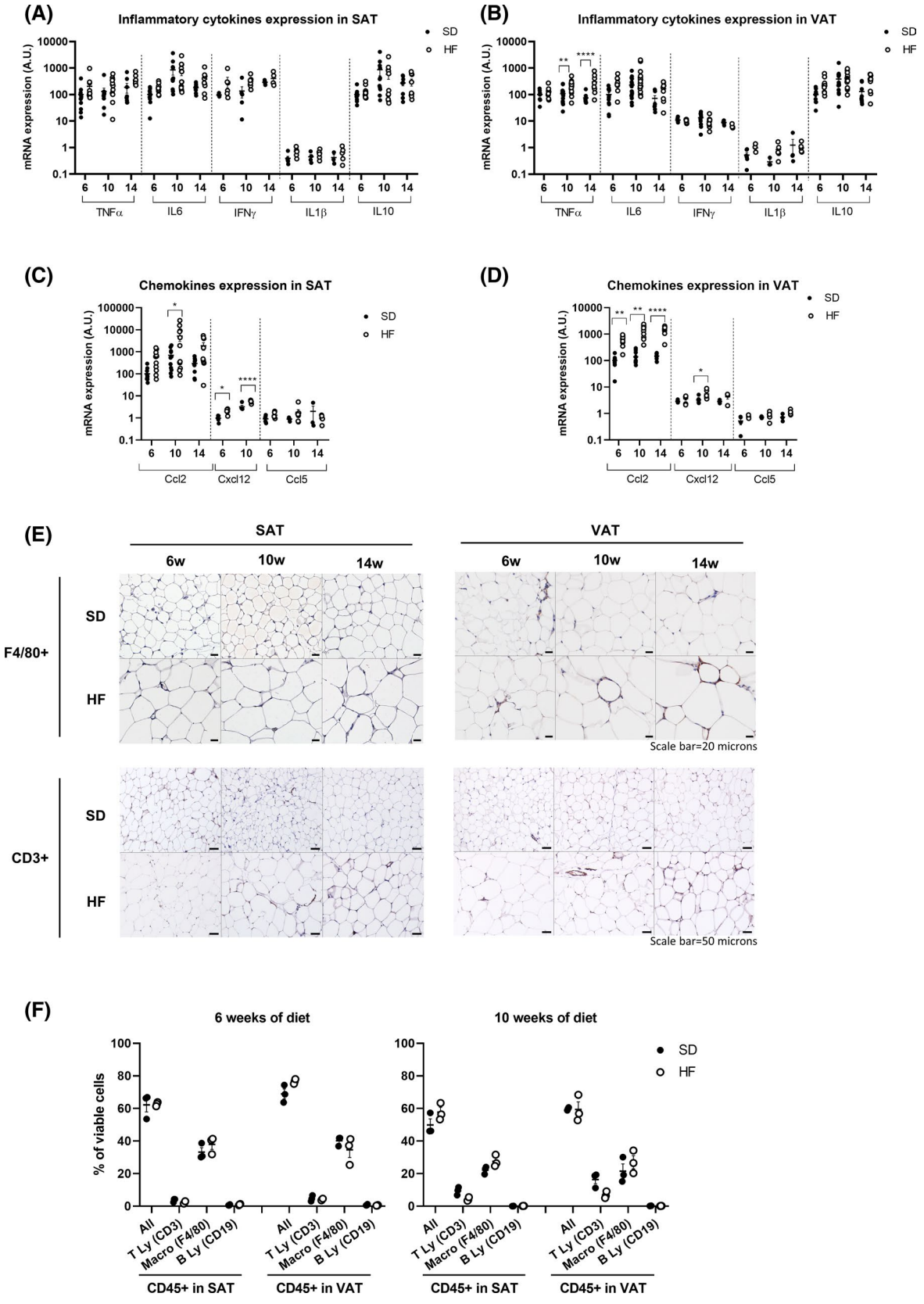

FIGURE 3 VAT was prone to inflammation earlier than SAT: A to D, The expression of mRNA levels in SAT and VAT were measured by RT-qPCR. Values calculated as in Figure 2 are in arbitrary units (AU). Mean ± SEM of n = 3 to 18 distinct mice identified by individual points. A, B, Expression of inflammatory cytokines in SAT and VAT, respectively, C, D, Expression of chemokines in SAT and VAT, respectively. Statistics are from two-way ANOVA followed by Sidak's test: $****P < 10^{-4}$, $***P < 10^{-3}$, $**P < .01$, $*P < .05$, n.s. not significant. E, Representative illustration of immunohistochemistry analysis to detect adipose tissue infiltration by macrophage (anti-F4/80 antibody) and by T lymphocytes (anti-CD3 antibody) in SAT and in VAT. F, Flow cytometry analysis of SAT and VAT stromal vascular fraction cleared of adipocytes and labeled with antibodies recognizing all the hematopoietic stem cells (CD45, All) and T lymphocytes (CD3, T Ly), macrophages (F4/80, Macro) or B lymphocytes (CD19, B Ly). Results represent the percent of each population among viable cells, each being also positive for CD45. Mean ± SEM from n = 3 distinct mice. Two-way ANOVA analysis revealed no statistical difference between SD and HF conditions

CD45 and CD31 (CD45- CD31-). The CD29 and CD90 positive cells (CD29+/CD90+) represented in average 67 to 79% of the cultured S-ASC and 64 to 77% of the V-ASC. This is in accordance with a previous study[23] and HF diet did not influence the distribution of these markers in vitro (Figure 4A). We also confirmed the higher cumulative number of cells obtained with S-ASC compared to V-ASC (Figure 4B) over 3 passages. This difference was poorly or not detectable when considering a single passage, as illustrated by the population doubling time represented in Figure S2 for cells collected at passage 3 after the seeding of the isolates and used for the experiments described in this study. We also confirmed the lower differentiation potential of V-ASC into adipocytes compared to S-ASC (Figure 4C). Despite signs of HF diet-dependent inhibition of S-ASC differentiation at isolated time-points (PPARγ, FAS, Adiponectin RNA) and a tendency to increase markers of V-ASC differentiation (DGAT2 and Adiponectin RNA) reflecting their plasticity, HF diet had no significant influence on any of the S- and V-ASC relative properties. This confirmed the adaptation period to obesity addressed in this study and the healthy status of ASC.[27]

3.3 | High-fat diet poorly and differently induces the expression of chemokines by S-ASC and V-ASC

Previous reports have shown that, in addition to cytokines involved in anti-inflammatory processes (IL10, HGF, TGFβ), ASC can be induced to secrete pro-inflammatory cytokines (IL6, IL8, TNFα) and chemokines, under the influence of a pro-inflammatory environment.[28-31] In basal conditions illustrated with SD diet, both S- and V-ASC expressed TNFα and HGF RNA and none expressed IL10 (Figure 5A). At the protein level, neither IL10, nor TNFα were detected in ASC conditioned media using ELISA assay (data not shown). Other cytokines revealed specific gene expression associated with the adipose depot of origin. IL6 was found in V-ASC only, while TGFβ transcripts were detected in S-ASC only (Figure 5A). ELISA assay confirmed the higher secretion of IL6 by V-ASC than S-ASC in basal conditions, with protein concentrations in V-ASC-conditioned media that were between 78- and 20-fold higher than in SD S-ASC-conditioned media after 6 and 10 weeks of SD diet, respectively (Figure 5B). Unexpectedly, TGFβ was found in both S- and V-ASC-conditioned media at similar levels but only after 14 weeks of feeding in basal conditions. The RNA expression of anti- and of pro-inflammatory cytokines was unchanged with HF diet in ASC isolated from both SAT and VAT in this kinetic protocol (Figure 5A), but protein analysis revealed HF diet-associated differences (Figure 5B). With HF diet, the secretion of IL6 by S-ASC was not induced while the mean concentration of IL6 in V-ASC-conditioned media was multiplied by about 7-, 24- and 16-fold compared to SD diet after 6, 10 and 14 weeks, respectively. After 14 weeks of feeding, the expression by V-ASC from SD fed mice presented an increased variability that abolished the statistical difference between the two groups. In S-ASC, HF diet induced the secretion of TGFβ after 10 and 14 weeks but differences with the SD group were not significant and of comparable concentration levels than in V-ASC-conditioned media despite lower transcriptional expression. These results reveal post-transcriptional regulation of IL6 production by V-ASC under the influence of HF diet (Figure 5B).

The expression of several chemokines, already reported to be expressed by mesenchymal stem cells, tended to be induced by the HF diet in V-ASC (Ccl5, Cxcl9, Ccl2, Cxcl10, Cxcl1) during the time course of the experiment, whereas in S-ASC, only one (Ccl5) was induced. All these inductions were of low intensity and not significant using multiple comparisons analysis, except for Cxcl1 in V-ASC after 14 weeks of feeding (Figure 5C).

Increased expression of chemokines and the recruitment of immune cells has been reported for MSC activated by inflammatory cytokines. This was associated with an increased potential to suppress activated T-cell proliferation[32] and the M1 polarization of macrophages.[33] To assess the activity of ASC on these cells, we performed Transwell migration assays and co-culture experiments with macrophages or with T lymphocytes in the presence of ASC.

3.4 | High-fat diet induces low-grade and isolated changes in the functional interaction of V-ASC, but not S-ASC, with macrophages

Macrophages are resident cells in healthy adipose tissue and macrophage infiltration occurs in obese conditions. For

attraction study, mouse RAW 264.7 macrophages were placed in the upper chamber of a Transwell device and ASC were seeded in the lower chamber. Results in Figure 6A show that the diet poorly influenced the attraction of macrophages by S-ASC but influenced V-ASC according to two-way ANOVA ($P < .05$) despite comparisons by pairs did not indicate significant differences between SD and HF diet at isolated timepoints. These results indicate that HF diet induced a low-grade increase of V-ASC chemotaxis toward macrophages that became significant when cumulated over time.

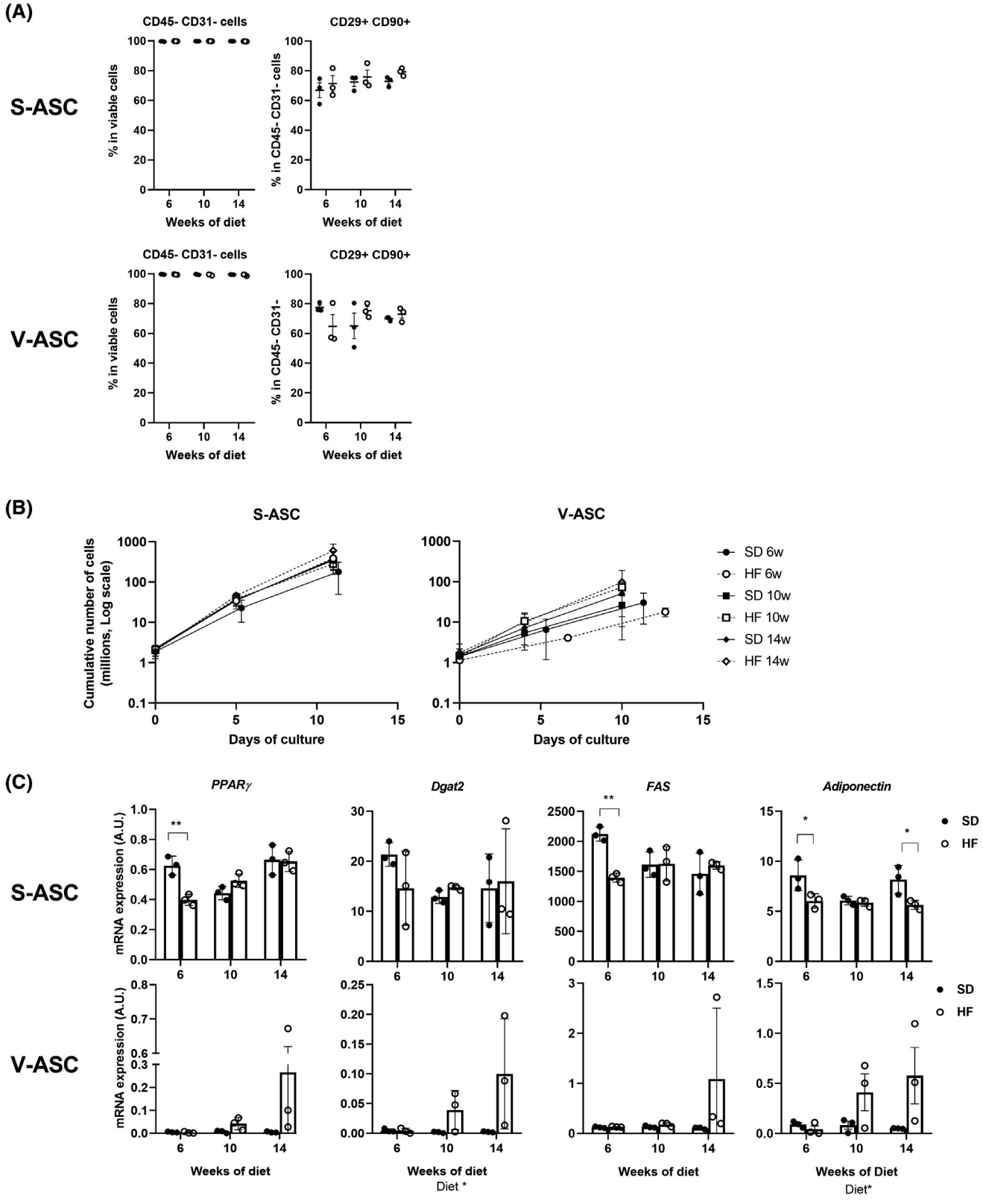

FIGURE 4 HF diet did not alter the membrane phenotype, the proliferation and the differentiation potential of cultured ASC: A, After collagenase dissociation of SAT and VAT and removal of the adipocytes, cells were plated and cultured for enrichment into ASC. Expression analysis of membrane markers by flow cytometry was performed after the third passage. Analysis was performed on viable cells that excluded the viability dye. Anti-CD45 and anti-CD31 antibodies were used to identify hematopoietic and endothelial cell lineages, respectively. All the cultured cells were negative for these lineage markers and the population was represented as Lin-. CD29 and CD90 are representative of mesenchymal stem cells and their co-expression is represented. Mean ± SEM from n = 3 distinct mice. B, Cumulative growth curves of S- and V-ASC using cell numeration over 3 passages. Mean ± SEM from n = 3 distinct mice. C, Expression of adipocyte differentiation markers by in vitro differentiated ASC, measured by RT-qPCR. Values calculated as in Figure 2 are in arbitrary units (AU). Mean ±SEM from n = 3 distinct animals. Statistics are from two-way ANOVA. Significant influence of HF in ANOVA is indicated by Diet* ($P < .05$) and was followed by Sidak's test for multiple comparisons. Only significant differences between SD and HF at each time-point are indicated as follow: $^{**}P < .01$, $^{*}P < .05$

In vivo and in vitro, ASC can switch the inflammatory macrophages (M1-like) towards an anti-inflammatory phenotype (M2-like), through the involvement of soluble factors.[34] To assess the effect of the diet on this property, LPS-activated murine RAW 264.7 cells were cultured for 24h in the presence of ASC-conditioned media from SD and HF diet fed mice. We measured by RT-qPCR, the expression by RAW cells of three markers of M1 polarization, IL1β, TNFα and iNOS that were efficiently induced by LPS treatment (Figure 6B, medium). In the presence of V- and S-ASC-conditioned media, incomplete and non-overlapping inhibitions were observed. Independently of the diet, S-ASC, but not V-ASC, inhibited the expression of IL1β by activated RAW cells, while the expression of TNFα was increased with diet duration. HF diet only influenced the properties of V-ASC that significantly inhibited TNFα expression by RAW cells after 6 and 10 weeks of HF diet. After 14 weeks of feeding, both SD and HF V-ASC inhibited TNFα expression by RAW cells. On other markers, the influence of the diet was not significant. The expression of iNOS was induced by LPS with variable intensity between experiments and the influence of S- and V-ASC was not reproducible, leading to non-significant differences with SD and HF diet. LPS-activation repressed the expression of M2 cytokines by RAW macrophages, such as IL10 and Arg1 that were difficult to detect. In the presence of ASC-conditioned media, their expression was not induced (Figure S3) confirming that alterations of the inflammatory cytokines pattern in LPS-activated macrophages were not representative of a M1 to M2 phenotype switch. We next analyzed ASC-conditioned media for the presence of two cytokines involved in M2 polarization, PGE2 and M-CSF. PGE2 is known to inhibit M1 polarization[30] and iNOS in LPS-activated RAW macrophages,[35] and was expressed by V-ASC but not by S-ASC. HF diet induced a significant but isolated increase of PGE2 concentration in V-ASC supernatant after 10 weeks of feeding. M-CSF involved in M2 polarization in the presence of IL10 and IL4,[28,31] was expressed by both ASC, but in V-ASC only, the secretion was increased with HF diet compared to SD after 6 and 10 weeks of feeding. Neither PGE2, nor M-CSF could explain the targeted inhibition of TNFα by V-ASC from HF diet fed mice, nor the difference observed between S- and V-ASC in the control of some and not all cytokines.

3.5 | With high-fat diet S-ASC, but not V-ASC, hamper the proliferation of activated T lymphocytes

T lymphocytes recruited in adipose tissue can be in a resting or in an activated state.[36] To explore the influence of ASC on both states, isolated T lymphocytes were directly seeded (resting) or first activated with anti-CD3 and anti-CD28 antibodies to mimic allogenic activation before seeding in the upper chamber of the Transwell device. We have counted and analyzed the migrated cells in the lower chamber containing ASC. Results in Figure 7A show that activated T lymphocytes spontaneously migrated toward the lower chamber but when S- or V-ASC were present, the number of migrating cells decreased. Analysis of the migrated cells did not show alterations in the relative proportions of CD4+ and CD8+ T lymphocytes or of regulatory T lymphocytes (CD4+, CD25+, FoxP3+) (Figure 7A). Resting T cells poorly migrated spontaneously and the presence of S- or V-ASC in the lower chamber had no effect (Figure 7A). These results revealed a new aspect of the immune regulation by ASC where S-ASC have a strong capacity to hamper the recruitment of activated T lymphocytes. This property was strengthened with the HF diet after 6 weeks of feeding and next with both the time and the diet to reach more than 70% of inhibition after 14 weeks of feeding. The inhibition by V-ASC was important (about 45%) but not influenced by the duration of the diet (Figure 7A).

ASC have anti-proliferative effect on T lymphocytes.[32] We used the method of CTV labeling decay to record, after 72 hours of culture, the fluorescence intensity of activated T lymphocytes and to measure the number of activated T lymphocytes accumulated at each round of division in the presence of ASC or not (Figure 7B, upper panel). Activated T lymphocytes cultured alone performed until 6 rounds of division with a maximum of the cells that divided 4 or 5 times. S- and V-ASC from SD diet fed mice efficiently decreased the proliferation of activated T lymphocytes when considering

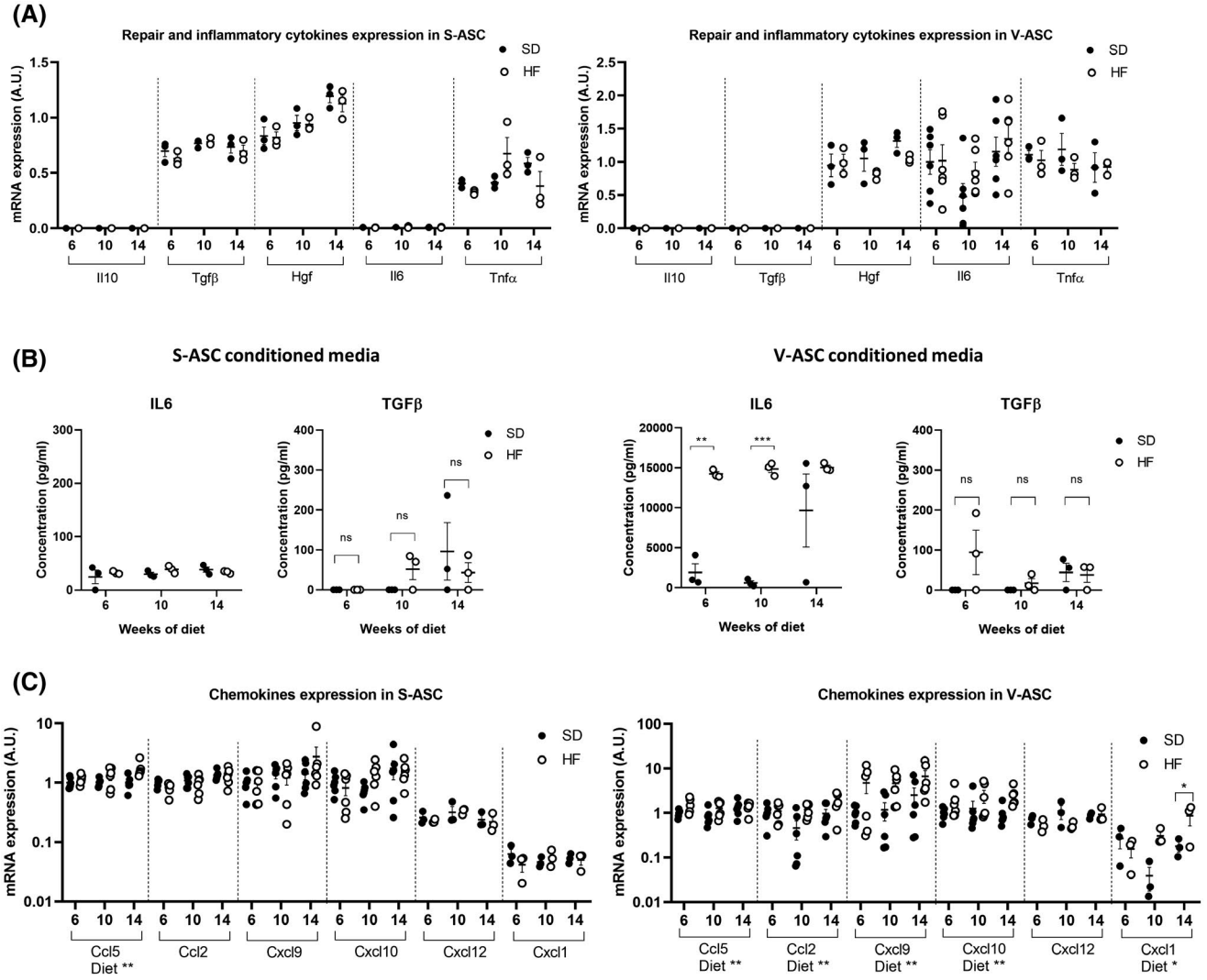

FIGURE 5 HF diet did not induce the expression of inflammatory cytokines by ASC but tended to increase the expression of chemokines in V-ASC: A, mRNA levels of cytokines expressed by S-ASC (left column) and V-ASC (right column) were quantified by RT-qPCR. IL10, TGFβ and HGF are repair cytokines while TNFα and IL6 are pro-inflammatory cytokines; IL8 that was not detectable in these samples is not represented. Values calculated as in Figure 2 are in arbitrary units (AU). Mean ± SD of n = 3 to 6 distinct mice, each was represented. For repair and pro-inflammatory cytokines, statistics from two-way ANOVA revealed no significant differences. For chemokines, statistics from two-way ANOVA indicated a significant influence of the HF diet compared to SD on the expression of several chemokines in V-ASC when considering the whole kinetic. It is indicated under the chemokine label by Diet $^{**}P < .01$ or $^{*}P < .05$, but no significant differences in comparisons by pairs using Sidak's test were observed on individual time-point. B, Concentration of IL6 and TGFβ in ASC conditioned media, measured by ELISA. Mean concentration ± SEM from n = 3 samples from distinct mice. Significant difference between SD and HF conditions is represented. C, mRNA levels of chemokines measured as described in (A). Statistics from two-way ANOVA followed by Sidak's tests: $^{***}P < 10^{-3}$, $^{**}P < .01$, $^{*}P < .05$, ns: not significant

the number of cells reaching this maximum of division. In both cases, T lymphocytes proliferation was slowed down by ASC from SD fed mice. Fluorescence intensities corresponded to a maximum of 2 or 3 divisions for the majority of the cells (Figure 7B, middle and lower panels), and a minority of cells with the maximal fluorescence intensity corresponding to undivided cell, were also observed in the presence of S-ASC but not V-ASC (division 0). Importantly, with S-ASC from 6 weeks HF fed mice, a drastic inhibition of T lymphocytes proliferation was observed with about 93% of the cells maintained in division 0 against 27% with SD diet S-ASC and 0.6% with T cells alone (medium). Longer exposures to the HF diet gave similar results (Figure 7B, upper and lower panel). Inhibition by V-ASC was observed only after 14 weeks of HF feeding and was more than 3-fold lower (26% in division 0) than with S-ASC. It is of note that cells

accumulated in division 0 were viable and had the morphology of activated T lymphocytes with increased size (FSC-A) and granulosity (SSC-A) (data not shown). Altogether, these results indicate that HF-activated S- and V-ASC inhibited activated T lymphocytes proliferation by distinct mechanisms, S-ASC acting with a higher efficiency by preventing most of the activated T lymphocytes from cell cycling.

Inhibition of activated T lymphocytes proliferation by ASC is a property shared with MSC. It is mediated by nitric oxide as the result of iNOS activity in MSC. iNOS activation requires IFNγ in combination with other pro-inflammatory cytokines such as TNFα. Chemokines, such as Cxcl9 and Cxcl10, secreted by activated MSC are also critical to this inhibitory effect since nitric oxide action requires proximity between MSC and T lymphocytes.[32] In the case of HF diet activated S-ASC, iNOS (Figure 7C) and chemokines (Figure 5C) were not induced suggesting alternative pathway. Other molecules already reported to manage activated T inhibition such as TGFβ1 and IL10,[37] or PTGS2 involved in the synthesis of PGE2,[38] have been examined in Figures 5 and 6 and were not induced by the HF diet. Finally we examined the expression of CD274 encoding for PD-L1 (Programmed death-ligand 1) reported to inhibit T lymphocytes proliferation by MSC upon activation by IFNγ.[39] PD-L1 was

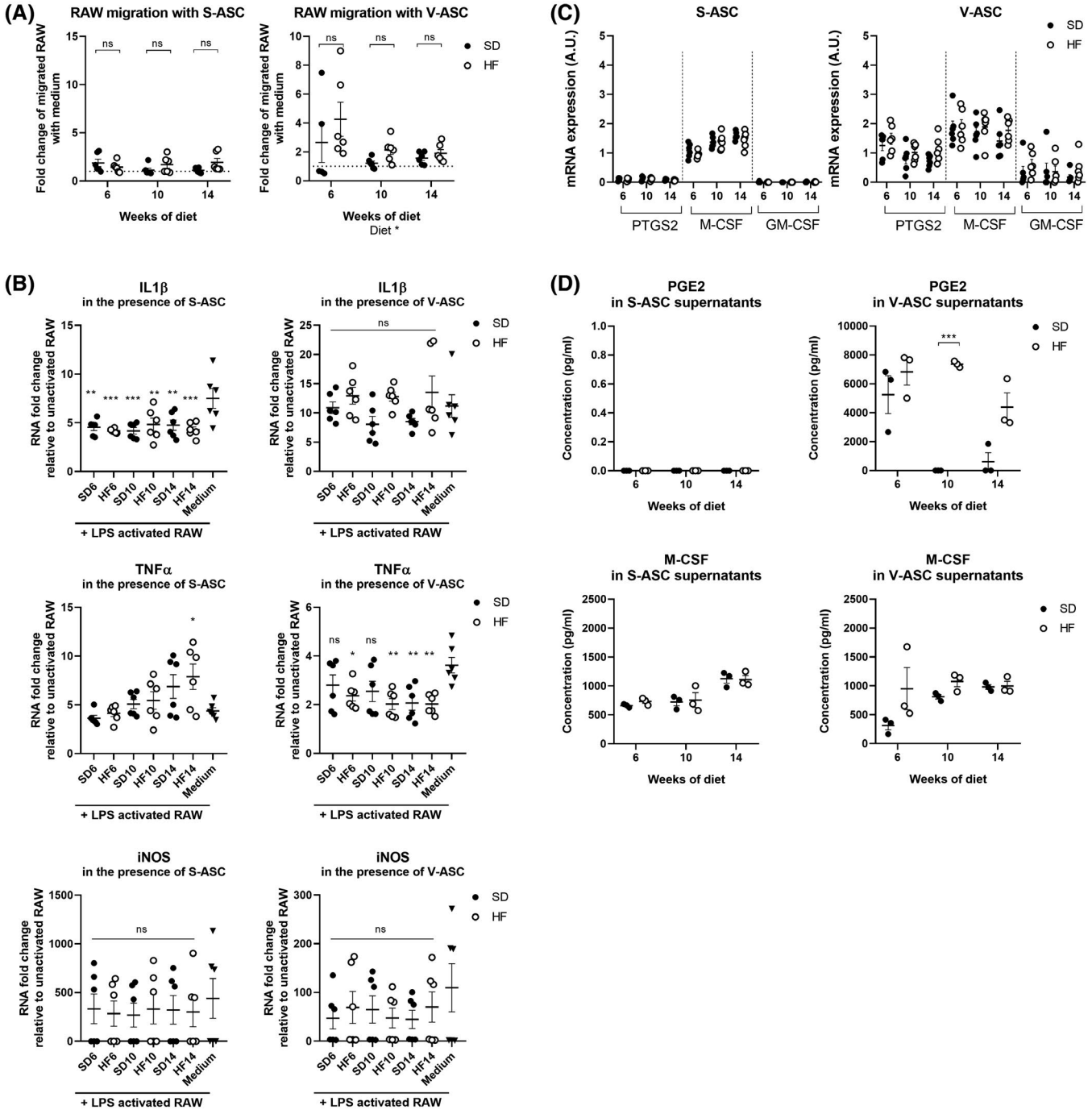

FIGURE 6 In V-ASC, but not in S-ASC, HF diet induced a low grade increase of macrophages attraction and a targeted inhibition of TNFα expression by activated RAW264.7 macrophages : A, Transwell migration assay: RAW264.7 macrophages placed into the upper chamber of the Transwell device were cultured in the presence of confluent layer of S-ASC and V-ASC isolated from mice fed HF or SD with HF diet for 6, 10 or 14 weeks. After 24h of culture, RAW cells that migrated through the Transwell were labeled with Hoechst and counted from image captures using ImageJ software. Fold changes of migrated RAW in the presence of ASC relative to the spontaneous migration in medium alone (represented with a dashed line at 1) are represented as mean ± SEM from n = 6 samples from distinct mice analysed in two independent experiments. Statistics from two-way ANOVA revealed significant difference between SD and HF conditions in the presence of V-ASC (Diet*, $P < .05$) but multiple comparisons by Sidak's tests indicated non-significant (ns) differences at individual time-points with both S- and V-ASC. B, RT-qPCR analysis of inflammatory genes expressed by LPS-activated RAW cells in the presence of S- and V-ASC conditioned media. mRNA expressions were calculated as in Figure 2 and divided by the result obtained with non-activated RAW cells cultured with medium alone to obtain fold changes that are represented as mean ± SEM, from n = 6 samples from distinct mice analysed in two independent experiments. Statistics are from one-way ANOVA followed by Dunnett's test for comparison with the fold change obtained with LPS alone (Medium). Results obtained for three inflammatory cytokines representative of the M1-like phenotype, TNFα, IL1β, and iNOS, are represented. C, RT-qPCR analysis of ASC for the expression of PTGS2 and M-CSF involved in the polarization of macrophages toward the M2 phenotype and of GM-CSF toward the M1 phenotype. Mean ± SEM from n = 6 samples from distinct mice. mRNA expressions calculated as in Figure 2 are in arbitray units (AU). D, Concentration of PGE2 and M-CSF in ASC-conditioned media, measured by ELISA. Mean concentration ± SEM from n = 3 samples from distinct mice are represented. Statistics are from two-way ANOVA followed by Sidak's tests and compared SD and HF conditions. *P*-values: $****P < 10^{-4}$, $***P < 10^{-3}$, $**P < .01$, $*P < .05$, ns: not significant

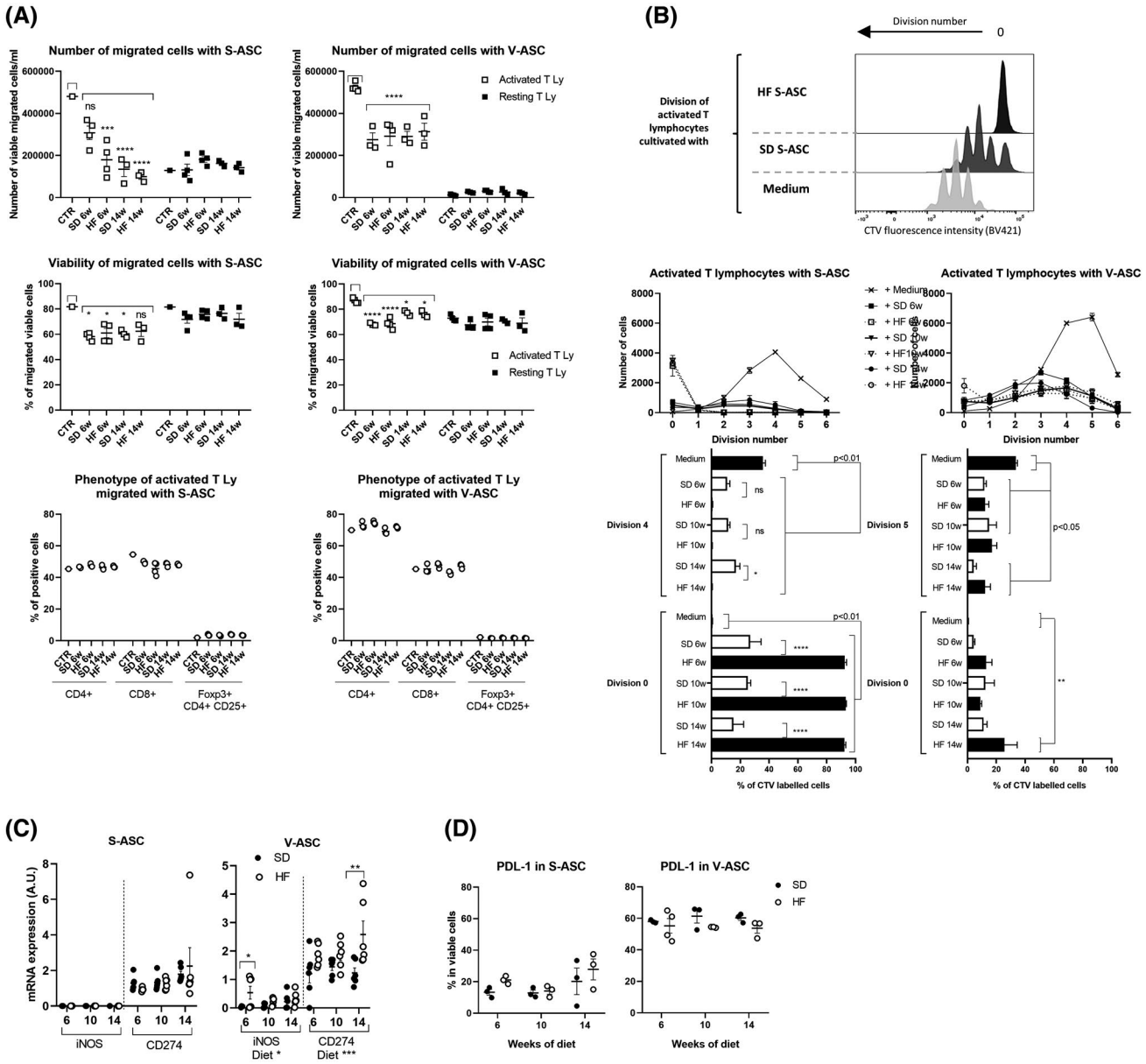

FIGURE 7 S-ASC from HF fed mice completely inhibited the proliferation of activated T lymphocytes and hampered their migration. A, Transwell migration assay: anti-CD3/anti-CD28-activated T lymphocytes were placed into the upper chamber of the Transwell device and cultured for 24h with S-ASC (left panels) and V-ASC (right panels) isolated from mice fed with HF or SD diet for 6, 10 or 14 weeks and at confluence. T lymphocytes were labeled with CTV before seeding. Migrated T lymphocytes into the lower chamber were labeled with a viable dye and with anti-CD3, CD4, CD8, CD25 and Foxp3 antibodies and analysed by flow cytometry. Results are mean ± SEM from n = 3 samples from distinct mice analyzed in duplicates. The upper panels represent the number of viable T lymphocytes that migrated into the lower chamber. The differences between SD and HF conditions were not significant but both S- and V-ASC significantly decreased the migration of activated T lymphocytes when compared to T cells alone (CTR). The middle panels show the % of viable T lymphocytes in the lower chamber compared to CTR. The lower panels show that the relative proportion of the viable T lymphocytes sub-populations that migrated into the lower chamber was maintained compared to CTR. B, ASC at subconfluency were cultured for 3 days with activated T lymphocytes labeled with CTV. Control was activated T lymphocytes cultured alone (Medium). The CTV decay was measured by flow cytometry. The spectral profiles of CTV obtained with activated LyT alone (Medium) or in coculture with 14 weeks HF and SD S-ASC are shown in the upper panel. They are representative of the results obtained at the other final time-point with S-ASC. In the middle panels, the number of cells accumulated at each round of division is represented by curves for all the conditions tested with S-ASC (left) and V-ASC (right). Curves with the same symbol are from the same kinetic-point and dash lines represent results obtained with HF ASC. In the lower panels, histograms represent the number of cells accumulated in the maximal round of division with T lymphocytes alone (division 4 in the experiment with S-ASC and 5 with V-ASC that were examined in distinct experiments), compared to the number of undivided T lymphocytes (division 0). In the absence of cell, some bars are represented but not visible. To facilitate the comparisons, results obtained with HF ASC and with the control cells are in black, while results with SD ASC are in white. Results are mean ± SEM from n = 3 samples from distinct mice and analyzed in triplicates. C, RT-qPCR analysis of ASC for the expression of iNOS and CD274 (encoding for the protein PD-L1) that have been involved in the inhibition of activated T lymphocytes by ASC activated with inflammatory cytokines. Values calculated as in Figure 2 are in arbitrary units (AU). Mean ± SEM from n = 6 distinct mice. Significant influence of the diet in two-way ANOVA is indicated with Diet* ($P < .05$) or Diet*** ($P < 10^{-3}$), D, Flow cytometry analysis of the membrane expression of PD-L1. Percent of PD-L1 expressing cells in viable cells are represented and are mean ± SEM from n = 3 samples from distinct mice. All the statistics are from two-way ANOVA followed by Sidak's test for multiple comparisons: ****$P < 10^{-4}$, ***$P < 10^{-3}$, **$P < .01$, *$P < .05$. Non-significant differences are either not indicated or indicated by ns

expressed by both S- and V-ASC as observed at the transcriptional level by RT-qPCR (CD274) and at the protein level by flow cytometry (Figure 7C,D respectively). The expression was higher in V-ASC than in S-ASC and was not influenced by the diet. Therefore, PD-L1 could explain the basal inhibition of activated T lymphocytes by S- and V-ASC in SD conditions but not the increased inhibition by S-ASC with HF diet. These results suggest the involvement of an unreported mechanism for the blockade of activated T lymphocytes by HF diet-activated S-ASC.

4 | DISCUSSION

The aim of this study was to determine whether obesity affects the interaction of ASC with immune cells before the onset of inflammation. Using a kinetic protocol of diet induced obesity, we examined ASC exposed in vivo to a systemic alteration of the glucose metabolism, in the absence of systemic inflammation measured by circulating IL6, TNFα, and MCP1, but sequentially associated (i) with non-inflammatory VAT and SAT, (ii) inflammatory VAT without insulin resistance and (iii) inflammatory VAT with insulin resistance, after 6, 10 and 14 weeks of HF feeding, respectively. Inflammatory cytokines were not detected in SAT during the time-course of this protocol. At the circulating level, the increase of PAI-1 after 10 weeks of HF diet correlated with the onset of VAT inflammation as described and is indicative of an increased risk of complications.[40] The increased circulating levels of the two adipokines, resistin and leptin, secreted by adipose tissue and the absence of major lipid metabolism alterations, reflect adaptation of adipose tissue to the increased energy supply. The proliferation and differentiation properties of S- and V-ASC were maintained and were typical of healthy cells. Therefore, this protocol addresses the functional adaptations of ASC to HF diet in an homeostatic process.

This study reveals that ASC are early sensors of metabolic alterations. They answer to HF diet by targeted and depot specific changes of their immunoregulating properties. The second feature of these changes is their induction from 6 weeks of HF feeding at a maximum level that was maintained thereafter. The third feature is the stability of these changes induced in vivo and maintained in vitro in ASC isolated from their inductive environment. These characteristics describe a process inducible by HF diet and promoting the acquisition, by healthy ASC, of new and definitive properties that were depot-specific.

In V-ASC, isolated from perigonadal adipose tissue, HF diet induced the specific release of IL6 in culture-conditioned media but not of TNFα, another inflammatory cytokine expressed at the transcriptional level. Circulating IL6 is mainly produced by VAT independent of obesity[41] and may support pro- and anti-inflammatory activities in adipose tissue[42] in addition to the stimulation of lipolysis and lipid oxidation.[43] Adipose tissue infiltration by recruited immune cells is an important feature of adipose tissue inflammation. Macrophage infiltration is an early event in VAT inflammation[20] that was not detected here. We show here that obesity

induced a discrete increase of V-ASC chemotaxis toward macrophages, typical of a low-grade contribution that over time, became significant. Macrophages are central in adipose tissue inflammation.[44] Cumulated with the release of IL6, V-ASC acquired with obesity features that may compose locally a pro-inflammatory context. Simultaneously, V-ASC acquired with obesity the potential to repress TNFα expression by LPS-activated macrophages, suggesting the secretion of an unidentified anti-inflammatory factor induced by HF diet. However, the increased expression of TNFα transcripts in VAT after 10 weeks of HF feeding suggest that V-ASC no longer controlled TNFα expression by resident VAT macrophages in vivo, probably activated by dead adipocytes in crown-like structures.[26]

Different from V-ASC, HF diet did not adjust the interaction of S-ASC with macrophages but rather increased their suppression of activated T lymphocytes. We observed that both S- and V-ASC similarly reduced the proliferation of activated T lymphocytes in basal condition but with HF diet, S-ASC only hampered the entry in division of activated T cells. This inhibition was not due to T cell death and did not involve the inhibitory mechanisms already reported for ASC exposed in vitro to inflammatory cytokines.[32,39] Adipose tissue resident T lymphocytes are important in the development of insulin resistance and inflammation, notably through the control of macrophages.[45] Our results show that S-ASC from obese mice stopped the proliferation of all the subsets of activated T lymphocytes, including the pro-inflammatory CD8+ cells,[46] the anti-inflammatory FoxP3+ Treg,[47] and CD4+ cells.[48] This property may support the observed absence of T lymphocytes and macrophages infiltration and of inflammation in SAT. With a lesser efficiency, V-ASC decreased the proliferation of activated T lymphocytes similarly to S-ASC in basal conditions; however, HF diet did not improve V-ASC activity. We also show here that S- and V-ASC inhibited T lymphocytes migration. Inhibition of activated T lymphocytes by V-ASC was maintained with HF diet and may account for the prevention of T lymphocytes infiltration in VAT. However, VAT homeostasis involves specific anti-inflammatory FoxP3+ Treg[16] and the lower inhibition of activated T lymphocytes by V-ASC compared to S-ASC, may indirectly prevent inflammation by maintaining the Treg subpopulation in SD and HF conditions.

The results presented here show that ASC are metabolic sensors adopting, in early obesity, targeted features to control activated macrophages in VAT and activated T lymphocytes in SAT. The HF-induced secretion of IL6 by V-ASC also suggests a rapid adaptation to energy overload by mobilizing already transcribed genes. The mechanisms involved occurred in vivo and remain to be understood. They probably result from metabolic activation, as already reported for immune cells.[49] Glucose metabolism was altered from 6 weeks of HF feeding and may represent a systemic activating factor, but local contact with lipids converging to adipose tissue for storage, may also account.

ASC isolated from inflammatory tissues in established obesity develop pro-inflammatory activities[29,50] and lose their differentiation potential,[51] suggesting that in vivo activated-ASC by inflammatory cytokines may not durably control the immune status of adipose tissue in obesity. Our results lead to the conclusion that immunoregulating properties of ASC are mobilized earlier in obesity, in answer to non-inflammatory signals, to engage these cells in the immune homeostasis of adipose tissue required for adaptation. We described here an obesity-primed immunocompetent state of ASC, stably acquired following exposure to obesity that differs from the activated state acquired in vitro following the exposure of naïve cells to inflammatory cytokines. This work places the activity of ASC in the immune adaptation of adipose depots to obesity and reveals ASC as new determinants of health in obesity.

AUTHOR CONTRIBUTIONS

CL, DC, TV, SC, AVM, SP, CP, JCF, AM performed investigations—CP, CL, DC provided resources—HV, AM, LG acquired funding—CL, AM, DC, LG designed the experimental methodology—CL, AM formatted the analysis and performed visualization for the article—AM, LG, HV supervised experiments, analyzed and validated the results—AM, CL wrote original draft—AM performed project conceptualization and administration. Anne Mey is the guarantor of this study and discloses no conflict of interest.

DATA AVAILABILITY STATEMENT

Data are available upon request.

ORCID

Camille Lefevre https://orcid.org/0000-0002-8508-7437
Jose Candido Ferraz https://orcid.org/0000-0002-0439-7098
Laurent Genestier https://orcid.org/0000-0002-0527-4583
Hubert Vidal https://orcid.org/0000-0002-9467-0317
Anne Mey https://orcid.org/0000-0002-2643-5702

REFERENCES

1. Hotamisligil GS. Inflammation and metabolic disorders. *Nature*. 2006;444(7121):860-867.
2. Caussy C, Wallet F, Laville M, Disse E. Obesity is associated with severe forms of COVID-19. *Obesity*. 2020;28(7):1175. http://dx.doi.org/10.1002/oby.22842
3. Duan Y, Zeng L, Zheng C, et al. Inflammatory links between high fat diets and diseases. *Front Immunol*. 2018;9:2649.
4. Cani PD, Bibiloni R, Knauf C, et al. Changes in gut microbiota control metabolic endotoxemia-induced inflammation in high-fat diet-induced obesity and diabetes in mice. *Diabetes*. 2008;57(6):1470-1481.

5. Reilly SM, Saltiel AR. Adapting to obesity with adipose tissue inflammation. *Nat Rev Endocrinol*. 2017;13:633-643.
6. Lin Y, Berg AH, Iyengar P, et al. The hyperglycemia-induced inflammatory response in adipocytes. *J Biol Chem*. 2005;280(6):4617-4626.
7. Patel PS, Buras ED, Balasubramanyam A. The role of the immune system in obesity and insulin resistance. *J Obes*. 2013;2013:616193.1–9.
8. Ding S, Chi MM, Scull BP, et al. High-fat diet: Bacteria interactions promote intestinal inflammation which precedes and correlates with obesity and insulin resistance in mouse. *PLoS One*. 2010;5:e12191. http://dx.doi.org/10.1371/journal.pone.0012191
9. Blüher M. Adipose tissue inflammation: a cause or consequence of obesity-related insulin resistance? *Clin Sci*. 2016;130:1603-1614.
10. McLaughlin T, Lamendola C, Liu A, Abbasi F. Preferential fat deposition in subcutaneous versus visceral depots is associated with insulin sensitivity. *J Clin Endocrinol Metab*. 2011;96(11):E1 756-E1760.
11. Alligier M, Gabert L, Meugnier E, et al. Visceral fat accumulation during lipid overfeeding is related to subcutaneous adipose tissue characteristics in healthy men. *J Clin Endocrinol Metab*. 2013;98:802-810.
12. Stolarczyk E. Adipose tissue inflammation in obesity: a metabolic or immune response? *Curr Opin Pharmacol*. 2017;37:35-40.
13. Fain JN, Madan AK, Hiler ML, Cheema P, Bahouth SW. Comparison of the release of adipokines by adipose tissue, adipose tissue matrix, and adipocytes from visceral and subcutaneous abdominal adipose tissues of obese humans. *Endocrinology*. 2004;145(5):2273-2282.
14. Rodeheffer MS, Birsoy K, Friedman JM. Identification of white adipocyte progenitor cells in vivo. *Cell*. 2008;135(2):240-249.
15. Kaundal U, Bagai U, Rakha A. Immunomodulatory plasticity of mesenchymal stem cells: a potential key to successful solid organ transplantation. *J Transl Med*. 2018;16:31.
16. Feuerer M, Herrero L, Cipolletta D, et al. Lean, but not obese, fat is enriched for a unique population of regulatory T cells that affect metabolic parameters. *Nat Med*. 2009;15:930-939.
17. Nishimura S, Manabe I, Takaki S, et al. Adipose natural regulatory B cells negatively control adipose tissue inflammation. *Cell Metab*. 2013;18(5):759-766.
18. Kulshrestha H, Gupta V, Mishra S, Mahdi AA, Awasthi S, Kumar S. Interleukin-10 as a novel biomarker of metabolic risk factors. *Diabetes Metab Syndr*. 2018;12(4):543-547.
19. Esposito K, Pontillo A, Giugliano F, et al. Association of low interleukin-10 levels with the metabolic syndrome in obese women. *J Clin Endocr Metab*. 2003;88:1055-1058.
20. Harman-Boehm I, Blüher M, Redel H, et al. Macrophage infiltration into omental versus subcutaneous fat across different populations: effect of regional adiposity and the comorbidities of obesity. *J Clin Endocr Metab*. 2007;92:2240-2247.
21. Lacasa D, Taleb S, Keophiphath M, Miranville A, Clement K. Macrophage-secreted factors impair human adipogenesis: Involvement of proinflammatory state in preadipocytes. *Endocrinology*. 2007;148:868-877.
22. Serena C, Keiran N, Ceperuelo-Mallafre V, et al. Obesity and type 2 diabetes alters the immune properties of human adipose derived stem cells. *Stem Cells*. 2016;34:2559-2573.
23. Lefevre C, Panthu B, Naville D, et al. Metabolic phenotyping of adipose-derived stem cells reveals a unique signature and intrinsic differences between fat pads. *Stem Cells Int*. 2019;2019:9323864.1–16.
24. Hammarstedt A, Gogg S, Hedjazifar S, Nerstedt A, Smith U. Impaired adipogenesis and dysfunctional adipose tissue in human hypertrophic obesity. *Physiol Rev*. 2018;98:1911-1941.
25. Bastard J-P, Piéroni L, Hainque B. Relationship between plasma plasminogen activator inhibitor 1 and insulin resistance. *Diabetes Metab Res Rev*. 2000;16(3):192-201.
26. Murano I, Barbatelli G, Parisani V, et al. Dead adipocytes, detected as crown-like structures, are prevalent in visceral fat depots of genetically obese mice. *J Lipid Res*. 2008;49(7):1562-1568.
27. Baptista LS, Silva KR, Borojevic R. Obesity and weight loss could alter the properties of adipose stem cells? *World Journal of Stem Cells*. 2015;7(1):165-173.
28. Kilroy GE, Foster SJ, Wu X, et al. Cytokine profile of human adipose-derived stem cells: expression of angiogenic, hematopoietic, and pro-inflammatory factors. *J Cell Physiol*. 2007;212(3): 702-709.
29. Lee MJ, Kim J, Kim MY, et al. Proteomic analysis of tumor necrosis factor-α-induced secretome of human adipose tissue-derived mesenchymal stem cells. *J. Proteome Res*. 2010;9(4):1754-1762.
30. Shirjang S, Mansoori B, Solali S, Hagh MF, Shamsasenjan K. Toll-like receptors as a key regulator of mesenchymal stem cell function: an up-to-date review. *Cell Immunol*. 2017;315:1-10.
31. Waterman RS, Tomchuck SL, Henkle SL, Betancourt AM. A new mesenchymal stem cell (MSC) paradigm: polarization into a pro-inflammatory MSC1 or an Immunosuppressive MSC2 phenotype. *PLoS One*. 2010;5:e10088.e10088. http://dx.doi.org/10.1371/journal.pone.0010088
32. Ren G, Zhang L, Zhao X, et al. Mesenchymal stem cell-mediated immunosuppression occurs via concerted action of chemokines and nitric oxide. *Cell Stem Cell*. 2008;2:141-150.
33. François M, Romieu-Mourez R, Li M, Galipeau J. Human MSC suppression correlates with cytokine induction of indoleamine 2,3-dioxygenase and bystander M2 macrophage differentiation. *Mol Ther*. 2012;20(1):187-195.
34. Shang Q, Bai Y, Wang G, et al. Delivery of adipose-derived stem cells attenuates adipose tissue inflammation and insulin resistance in obese mice through remodeling macrophage phenotypes. *Stem Cells Dev*. 2015;24(17):2052-2064.
35. Harbrecht BG, Kim Y-M, Wirant EA, Simmons RL, Billiar TR. Timing of prostaglandin exposure is critical for the inhibition of LPS- or IFN-γ-induced macrophage NO synthesis by PGE2. *J Leukoc Biol*. 1997;61(6):712-720.
36. Wang Q, Wu H. T Cells in adipose tissue: critical players in immunometabolism. *Front Immunol*. 2018;9. https://doi.org/10.3389/fimmu.2018.02509
37. Nasef A, Chapel A, Mazurier C, et al. Identification of IL-10 and TGF-β transcripts involved in the inhibition of T-lymphocyte proliferation during cell contact with human mesenchymal stem cells. *Gene Expr*. 2018;13(4):217-226.
38. Yañez R, Oviedo A, Aldea M, Bueren JA, Lamana ML. Prostaglandin E2 plays a key role in the immunosuppressive properties of adipose and bone marrow tissue-derived mesenchymal stromal cells. *Exp Cell Res*. 2010;316(19):3109-3123.
39. Chinnadurai R, Copland IB, Patel SR, Galipeau J. IDO-independent suppression of T cell effector function by IFN-γ-licensed human mesenchymal stromal cells. *J Immunol*. 2014;192(4):1491-1501.

40. Serrano R, Barrenetxe J, Orbe J, et al. Tissue-specific PAI-1 gene expression and glycosylation pattern in insulin-resistant old rats. *Am J Physiol-Regul, Integr Comp Physiol*. 2009;297:R1563-R1569.
41. Antuna-Puente B, Feve B, Fellahi S, Bastard J-P. Adipokines: the missing link between insulin resistance and obesity. *Diabetes Metab*. 2008;34(1):2-11.
42. Han MS, White A, Perry RJ, et al. Regulation of adipose tissue inflammation by interleukin 6. *Proc Natl Acad Sci USA*. 2020;117(6):2751-2760.
43. Vernon RG, Denis RGP, Sørensen A. Signals of adiposity. *Domest Anim Endocrinol*. 2001;21:197-214.
44. Solinas G, Vilcu C, Neels JG, et al. JNK1 in hematopoietically derived cells contributes to diet-induced inflammation and insulin resistance without affecting obesity. *Cell Metab*. 2007;6(5):386-397.
45. Chatzigeorgiou A, Karalis KP, Bornstein SR, Chavakis T. Lymphocytes in obesity-related adipose tissue inflammation. *Diabetologia*. 2012;55(10):2583-2592.
46. Nishimura S, Manabe I, Nagasaki M, et al. CD8 + effector T cells contribute to macrophage recruitment and adipose tissue inflammation in obesity. *Nat Med*. 2009;15:914-920.
47. Feuerer M, Herrero L, Cipolletta D, et al. Fat Treg cells: a liaison between the immune and metabolic systems. *Nat Med*. 2009;15:930-939.
48. Winer S, Chan Y, Paltser G, et al. Normalization of obesity-associated insulin resistance through immunotherapy. *Nat Med*. 2009;15:921-929.
49. Kratz M, Coats BR, Hisert KB, et al. Metabolic dysfunction drives a mechanistically distinct proinflammatory phenotype in adipose tissue macrophages. *Cell Metab*. 2014;20(4):614-625.
50. Eljaafari A, Robert M, Chehimi M, et al. Adipose tissue-derived stem cells from obese subjects contribute to inflammation and reduced insulin response in adipocytes through differential regulation of the Th1/Th17 balance and monocyte activation. *Diabetes*. 2015;64(7):2477-2488.
51. De Girolamo L, Stanco D, Salvatori L, et al. Stemness and osteogenic and adipogenic potential are differently impaired in subcutaneous and visceral adipose derived stem cells (ASCs) isolated from obese donors. *Int J Immunopathol Pharmacol*. 2013;26(1_suppl):11-21.

SUPPORTING INFORMATION

Additional Supporting Information may be found online in the Supporting Information section.

How to cite this article: Lefevre C, Chartoire D, Ferraz JC, et al. Obesity activates immunomodulating properties of mesenchymal stem cells in adipose tissue with differences between localizations. *The FASEB Journal*. 2021;35:e21650. https://doi.org/10.1096/fj.202002046RR